British Journal of Pharmacology (2007) 151, 483–493
 0007–1188/07 $30.00
www.brjpharmacol.org

RESEARCH PAPER

Non-steroidal anti-inflammatory drugs increase insulin release from beta cells by inhibiting ATP-sensitive potassium channels

J Li[1,2], N Zhang[3], B Ye[1], W Ju[4], B Orser[2,4], JEM Fox[4], MB Wheeler[4], Q Wang[3,4] and W-Y Lu[1,2,4]

[1]*Department of Anesthesia, Sunnybrook Health Sciences Centre, University of Toronto, Toronto, Ontario, Canada;* [2]*Department of Anesthesia, University of Toronto, Toronto, Ontario, Canada;* [3]*Division of Endocrinology & Metabolism, St Michael's Hospital, University of Toronto, Toronto, Ontario, Canada and* [4]*Department of Physiology, University of Toronto, Toronto, Ontario, Canada*

Background and purpose: Some non-steroidal anti-inflammatory drugs (NSAIDs) incidentally induce hypoglycemia, which is often seen in diabetic patients receiving sulphonylureas. NSAIDs influence various ion channel activities, thus they may cause hypoglycemia by affecting ion channel functions in insulin secreting beta cells. This study investigated the effects of the NSAID meclofenamic acid (MFA) on the electrical excitability and the secretion of insulin from pancreatic beta cells.
Experimental approach: Using patch clamp techniques and insulin secretion assays, the effects of MFA on the membrane potential and transmembrane current of INS-1 cells, and insulin secretion were studied.
Key results: Under perforated patch recordings, MFA induced a rapid depolarization in INS-1 cells bathed in low (2.8mM), but not high (28mM) glucose solutions. MFA, as well as acetylsalicylic acid (ASA) and flufenamic acid (FFA), excited the cells by inhibiting ATP-sensitive potassium channels (K_{ATP}). In whole cell recordings, K_{ATP} conductance consistently appeared when intracellular ATP was diluted. Intracellular glibenclamide prevented the development of K_{ATP} activity, whereas intracellular MFA had no effect. At low glibenclamide concentrations, MFA induced additional inhibition of the K_{ATP} current. Live cell Ca^{2+} imaging displayed that MFA elevated intracellular Ca^{2+} at low glucose concentrations. Furthermore, MFA dose-dependently increased insulin release under low, but not high, glucose conditions.
Conclusions and Implications: MFA blocked K_{ATP} through an extracellular mechanism and thus increased insulin secretion. As some NSAIDs synergistically inhibit K_{ATP} activity together with sulphonylureas, the risk of NSAID-induced hypoglycemia should be considered when glucose-lowering compounds are administered.
British Journal of Pharmacology (2007) **151,** 483–493; doi:10.1038/sj.bjp.0707259; published online 16 April 2007

Keywords: NSAID; meclofenamic acid; K_{ATP}; INS-1 cells; Ca^{2+}; insulin secretion

Abbreviations: ASA, acetylsalicylic acid; COX, cyclooxygenase; $[Ca^{2+}]_i$, intracellular Ca^{2+} concentration; ECS, extracellular solution; FFA, flufenamic acid; ICS, intracellular solution; K_{ATP} channel, ATP-sensitive potassium channel; MFA, meclofenamic acid; NSAID, non steroid anti-inflammatory drug; PTXN, picrotoxin; SUR, sulphonylurea receptor; V_M, membrane potential

Introduction

Nonsteroidal anti-inflammatory drugs (NSAIDs), such as acetylsalicylic acid (ASA), ibuprofen, flufenamic acid (FFA) and meclofenamic acid (MFA) are widely used medications because they provide effective relief of chronic pain and inflammation via inhibition of cyclooxygenase (COX). It has also long been known that high doses of salicylates lower plasma glucose concentrations (Reid *et al*., 1957; Gilgore and Rupp, 1961; Baron, 1982; Kubacka *et al*., 1996). In addition, some NSAIDs, for example, ibuprofen (Sone *et al*., 2001) can incidentally induce hypoglycemia in diabetic patients who receive sulphonylurea therapy. However, the underlying mechanism(s) through which NSAIDs affect plasma levels of glucose remain unclear.

With regard to the regulation of glucose metabolism in pancreatic beta cells, ATP-sensitive K^+ (K_{ATP}) channels function as a molecular sensor of cellular metabolism and play a critical role in regulation of insulin secretion from the beta cells (Nichols, 2006). The ATP-sensitive potassium channels (K_{ATP}) channels in beta cells are hetero-octamers composed of two different subunits, four inwardly rectifying K^+ channel subunits (Kir6.2) and four sulphonylurea

Correspondence: Dr W-Y Lu, Sunnybrook Health Sciences Centre, University of Toronto, Room S104, 2075 Bayview Avenue, Toronto, Ontario, Canada M4N 3M5.
E-mail: weiyang.lu@sw.ca
Received 10 January 2007; revised 5 March 2007; accepted 13 March 2007; published online 16 April 2007

receptors (SUR1) (Gloyn *et al*., 2006). The activity of K_{ATP} channels is effectively regulated by the ratio of intracellular ATP to ADP. During glucose metabolism, increased intracellular ATP inhibits channel activity, leading to membrane depolarization and insulin secretion (Gloyn *et al*., 2006; Nichols, 2006). In beta cells, the increased ATP can also open transient receptor potential channels (Qian *et al*., 2002; Kawajiri *et al*., 2006), a family of nonselective cation channels that are permeable to Ca^{2+}. Moreover, increased glucose triggers an anionic flux by activating a volume-sensitive Cl^- channel in the beta cells (Kinard and Satin, 1995; Best, 2002, 2005). Together, these ion channel activities regulated by glucose metabolism effectively control the excitability of beta cells and hence the secretion of insulin.

NSAIDs could have an effect on plasma glucose levels by affecting ion channel functions in pancreatic beta cells and, consequently, insulin secretion. For instance, MFA is a known opener of KCNQ2/Q3 K^+ channels (Peretz *et al*., 2005), but an inhibitor of Kv2.1 channels (Lee and Wang, 1999). More to the point, MFA might be a K_{ATP} channel blocker, as it reduced the cardioprotective effect of the K_{ATP} opener cromakalim (Grover *et al*., 1994). The present study sought to investigate the underlying mechanisms for the hypoglycaemic action of some NSAIDs. We tested the hypothesis that NSAIDs induce hypoglycemia by increasing insulin release from pancreatic beta cells. Specifically, we examined the effects of MFA on the membrane conductance of INS-1 cells, a widely used pancreatic beta cell line, and on insulin secretion from these cells. Our data demonstrated that MFA increases insulin release from INS-1 cells by inhibiting the K_{ATP} channels.

Methods

Cell culture

INS-1 cells (passages 50–65) were maintained in RPMI 1640 medium (Invitrogen, Burlington, Ontario, Canada) containing fetal bovine serum (10% v/v), 100 U ml^{-1} penicillin G sodium, 100 μg ml^{-1} streptomycin sulphate, 110 mg l^{-1} sodium pyruvate, 2.28 g l^{-1} HEPES and 3.4 μl l^{-1} β-mercaptoethanol at 37°C in an atmosphere of humidified air (95%) and CO_2 (5%).

Isolation of pancreatic beta cells

Islets of Langerhans were isolated from the mouse insulin I gene promoter (MIP)-GFP-transgenic mice as described previously (Hara *et al*., 2003; Dai *et al*., 2006). Briefly, saline containing 0.8 mg ml^{-1} collagenase (type V; Sigma, St Louis, MO, USA) was injected into the pancreatic duct to expand the pancreas. The inflated pancreas was removed, incubated at 37°C for 20 min and shaken vigorously to disrupt the tissue. The islets were then collected by hand picking. To obtain single islet cells, the intact mouse islets were dispersed in dispase II solution (Roche Diagnostics, GmbH, Germany) at 37°C for 5 min and the single cells were plated on glass coverslips. The intact islets and single islet cells were cultured in RPMI 1640 medium containing 11.1 mM glucose supplemented with 10% fetal bovine serum, 10 mM HEPES, 100 units ml^{-1} penicillin and 100 μg ml^{-1} streptomycin for 24–72 h before experiments.

Electrophysiology

Perforated or conventional whole cell patch-clamp recordings were performed in INS-1 cells using an Axopatch-1D amplifier (Axon Instruments, Foster City, CA, USA). Before being used for recordings, the cells were bathed in the standard extracellular solution (ECS) containing (in mM) 145 NaCl, 1.3 $CaCl_2$, 5.4 KCl, 25 HEPES (pH 7.4), at 36°C, for 30 min. In accordance with experimental designs, ECS was made with three different concentrations (0, 2.8 and 28 mM) of glucose. Electrodes (3–5 MΩ) were constructed from thin-walled glass (1.5 mm diameter; World Precision Instruments, Sarasota, FL, USA) using a two-stage puller (PP-830, Narishige, East Meadow, NY, USA). The standard intracellular solution (ICS) for perforated patch recording consisted of (in mM) 150 KCl, 10 HEPES, 2 $MgCl_2$ and 1 $CaCl_2$. After addition of the pore-forming agent gramicidin (50 μg ml^{-1}, Sigma-Aldrich Corp., Buchs, Switzerland) (Sugita *et al*., 2004), the pH of the ICS was adjusted to 7.30 (with KOH) and the osmolarity was corrected to a range of 310–315 mOsM. Perforated patch recordings started under voltage-clamp mode. The membrane perforation was observed as a constant decrease in serial resistance after electrode seal. In most of the recordings, the resistance declined to a value ranging from 30 to 35 MΩ within 5–15 min after the seal, and then the resistance stabilized for about 40–80 min. To monitor a possible formation of whole cell configuration, the serial resistance was examined approximately every 5 min during the recording. Recordings showing a sudden change in the resistance were abandoned and not used for the study. For specific experiments, whole cell recordings were also performed in INS-1 cells. In some whole cell recordings, the ICS components were changed as described in the Results. All the electrical signals were digitized, filtered (1 kHz) and acquired online using Clampex software and analysed offline using Clampfit software (Axon Instruments).

NSAIDs were focally applied to the recorded cell using a computer-controlled multibarreled perfusion system (SF-77B, Warner Instruments, Hamden, CT, USA). To study the effect of NSAIDs on the excitability of INS-1 cells, changes in the membrane potential (V_M) were recorded under current-clamp mode. To determine which transmembrane conductance was affected by NSAIDs, transmembrane currents were elicited by hyperpolarizing or depolarizing voltage steps (for example in Figure 2a), or by a voltage-ramp (V-ramp, a steady voltage change from −80 to 60 mV within 1.5 s, for example in Figure 2c). The V_M value was measured using a 2 s sample obtained immediately before and during the last 2 s of drug application. The 2 s sample was averaged and used for analysis.

Live-cell fluorescent imaging

For this assay, INS-1 cells were cultured on 25 mm glass coverslips coated with poly-D-lysine (Sigma) for 2 days. Before use, cells were bathed in ECS containing 2.8 or 28 mM glucose at 36°C for 30 min. At the same time, cells were

loaded with Fluo4 Ca^{2+}-sensitive dye (Invitrogen, 0.5 μM, 30 min). For Ca^{2+} imaging, the cell culture coverslip was rinsed and inserted into a live-cell recording chamber (Attofluor chamber, Invitrogen) and then immersed in 1 ml extracellular fluid (ECF; with 2.8 or 28 mM glucose). Cells were visualized under a $\times 60$ oil-immersion lens using an Evolution QEi CCD digital camera attached to an Olympus microscope system driven by Image-Pro software (Media Cybernetics, Bethesda, MD, USA). Images of live cells were acquired at 2 s intervals using Image-Pro software. Acquired bright-field images were enhanced using the Enhance Display options where all images were adjusted to account solely for differences in the background levels of light. Basal Ca^{2+} signal was visualized for 2–3 min before the application of the testing reagents to the ECS. The intensity of the Ca^{2+} signal was analysed using the Image J program (National Institutes of Health, Bethesda, MD, USA) and normalized to the basal level.

Insulin secretion

Insulin concentrations were measured as described previously (Wang *et al*., 2004). Briefly, INS-1 cells grown in 24-well plates to 85–90% confluency were rinsed twice and incubated with Krebs-Ringer bicarbonate buffer (KRB, in mM) containing 115 NaCl, 5 KCl, 24 $NaHCO_3$, 2.5 $CaCl_2$, 1 $MgCl_2$, 10 HEPES and 0.1% bovine serum albumin for 60 min. Cells were incubated in KRB in the presence of various concentrations of glucose and/or NSAIDs (Sigma Chemical, St Louis, MO, USA) as indicated. After 30 min of incubation at 37°C in an atmosphere of humidified air (95%) and CO_2 (5%), the media were collected and insulin concentrations were measured by radioimmunoassay using the rat insulin RIA kit (Linco Research Inc., St Charles, MO, USA). The insulin secretion was normalized to the cellular protein content. Proteins were determined using the Bio-Rad protein assay kit (Bio-Rad Laboratories, CA, USA).

Statistical analysis

Analysis of electrophysiological data was performed using the Clampfit program (pClamp 8.1; Axon Instruments). In the dose–response curve, each data point represented the mean value of responses from several experiments, and the curves were obtained by fitting the data using an equation as below:

$$y = E_{\mathrm{Min}} + E_{\mathrm{Max}}/(1 + [D/\mathrm{EC}_{50}])^{\mathrm{Hill}}$$

In the equation, y is the delta change of responses to the testing compound, E_{Min} is the minimum response and E_{Max} is the maximum response in the presence of different concentrations of the compound; D is the testing concentration of the compound; EC_{50} (IC_{50}) is the concentration of the drug that produced 50% of the maximum effect. Hill is the Hill coefficient.

Data was expressed as mean $\pm$ s.e.m. Means were compared with Student's unpaired or paired t-test where appropriate using the SigmaStat software from Jandal Scientific Co. A P-value <0.05 was considered as significant.

Results

MFA depolarizes INS-1 cells at low concentrations of glucose

We reasoned that if NSAIDs influence insulin release by regulating ion channel activities, they should regulate the excitability of beta cells. We therefore made perforated patch recordings in INS-1 cells and examined the V_M of the cells at different concentrations of extracellular glucose. Under current–clamp recordings, increasing glucose induced a membrane depolarization in INS-1 cells in a concentration-dependent manner (Figure 1a). Most tested cells generated action potentials that were superimposed on the glucose-induced depolarization (Figure 1a, inset). Collected data showed that at low glucose INS-1, cells displayed a hyperpolarized and stable V_M, whereas at high concentrations of glucose the cells exhibited depolarized V_M (Figure 1b). Notably, INS-1 cells displayed larger fluctuations of V_M at high glucose than that at low glucose (Figure 1c).

MFA is a common clinically used NSAID. We examined effects of MFA on the V_M of INS-1 cells at low and high glucose. MFA induced depolarization in the beta cells at 0 and 2.8mM glucose (Figure 1d and e) in a dose-dependent manner (Figure 1g and h; EC_{50} at 0 mmol l^{-1} G: 29.2 μM, $n=5$; at 2.8 mM G: 24.6 μM). In another set of experiments carried out in the presence of 0 mM glucose, 5 out of 9 tested cells displayed membrane depolarization in response to 1.0 μM MFA (0.7 ± 0.05 mV, $n=5$; in comparison to the basal V_M fluctuation, $P<0.05$), and all tested cells were depolarized when exposed to 3.0 μM MFA (1.6 ± 0.4 mV, $n=9$; in comparison to the basal V_M fluctuation, $P<0.01$).

Pancreatic beta cells release γ-aminobutyric acid (GABA) (Solimena, 1998) and express functional A-type GABA receptors (Dong *et al*., 2006). Thus, beta cells contain an excitatory autocrine or paracrine signalling system. Since MFA enhances the activity of $GABA_A$Rs recombinantly expressed in oocytes (Woodward *et al*., 1994), we investigated whether MFA excites beta cells by upregulating the function of $GABA_A$ receptors. Notably, the MFA-induced depolarization persisted in the presence of the $GABA_A$ receptor antagonist bicuculline (not shown) or picrotoxin (PTXN; Figure 1j). In contrast, MFA showed no effect on the V_M of those cells that were incubated in 28 mM glucose (Figure 1f and i). Considering that MFA can up- and downregulate various ion channel functions (Ottolia and Toro, 1994; Woodward *et al*., 1994; Lee and Wang, 1999; Harks *et al*., 2001; Peretz *et al*., 2005), we proposed that MFA could stimulate the cells either by inhibiting an outward conductance that is active in the presence of low glucose (for example, K_{ATP}), or by opening an inward conductance that is inactivated by low glucose (for instance, the volume-sensitive Cl^- channel (Kinard and Satin, 1995; Best, 2002, 2005)).

We characterized the transmembrane current of INS-1 cells in the presence of different glucose concentrations (0, 2.8 or 28 mM). Specifically, under perforated patch voltage-clamp recording conditions the currents were elicited by hyperpolarizing and depolarizing voltage steps (Figure 2a). Analysis of the current–voltage (I–V) relationship revealed that in the presence of 28 mM of glucose the voltage-step evoked currents in INS-1 increased abruptly when the membrane

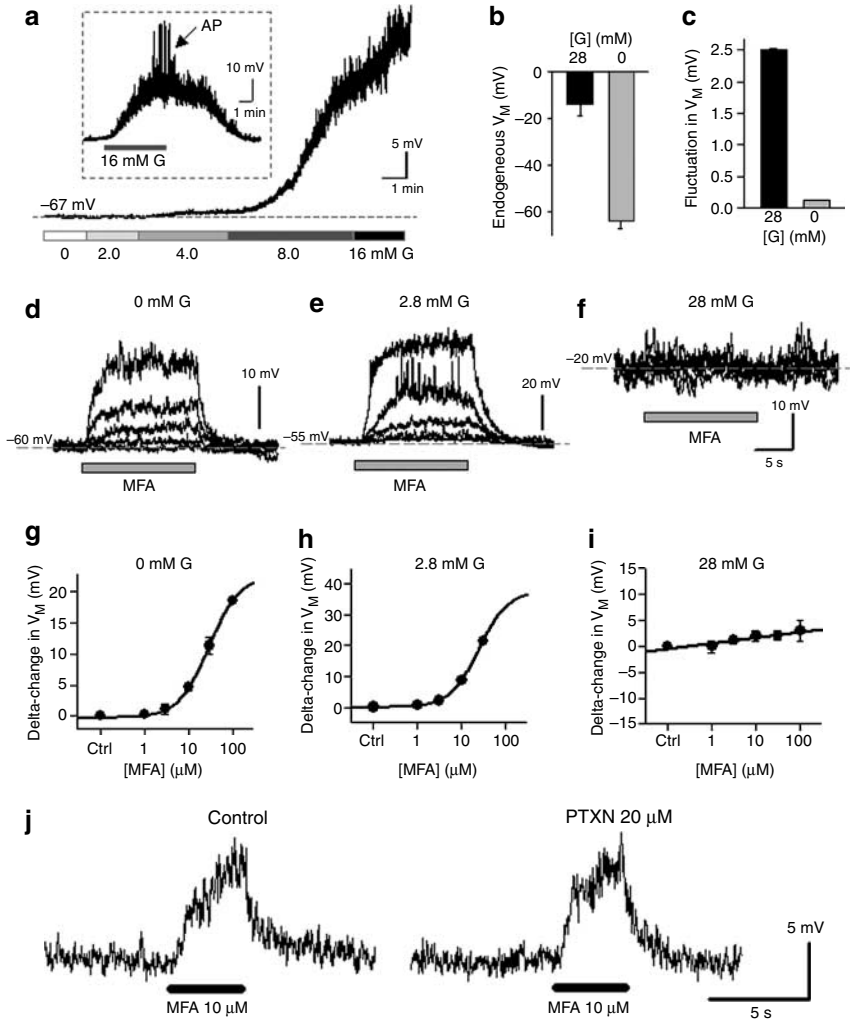

Figure 1 MFA induces membrane depolarization in INS-1 cells at low extracellular glucose. All results shown in the figure were obtained by perforated patch recordings. (**a**) Glucose dose-dependently induces membrane depolarization. Inset: some cells generate action potentials during glucose-induced depolarization. (**b**) The average V_M of INS-1 cells was depolarized in the presence of 28 mM extracellular glucose (*G*), relative to that in glucose-free (0 mM) solution ($n=7$; $P<0.001$). (**c**) The fluctuation amplitude of V_M was higher in the presence of 28 mM glucose than in glucose-free ECF ($n=8$; $P<0.001$). In (**d**) and (**g**), MFA dose-dependently induces depolarization in the presence of 0 mM or (**e** and **h**) of 2.8 mM of glucose, but not at 28 mM of glucose (**f** and **i**). Typical traces in (**d**–**f**) show the effects of 1, 3, 10, 30 and 100 μM of MFA on the V_M of cells in the presence of low and high glucose, respectively. Note that the V_M is at a highly depolarized level when the cell is bathed in high glucose, and that the EC_{50} values of MFA-induced membrane depolarization are similar at 0 and 2.8 mM glucose. (**j**) MFA readily depolarizes the cells in the presence of 20 μM of PTXN.

was depolarized to levels above −20 mV (Figure 2a1), representing a voltage-dependent conductance (Figure 2b). When the cell was bathed in glucose-free solution, the amplitudes of currents evoked by each voltage-step were increased (Figure 2a2 and b), implying the development of a non-voltage-dependent conductance (NVDC). The profile of the glucose-sensitive conductance in the cells could also be characterized by changing the cellular V_M via a voltage ramp (V-ramp) (Figure 2c). The component of glucose-sensitive conductance was obtained by subtracting the current evoked at 28 mM glucose from the current elicited in the absence of glucose, which showed a linear *I–V* relationship (Figure 2c) and thus demonstrated that it is an NVDC. Notably, application of MFA to the cells suppressed the glucose-sensitive NVDC (Figure 2d1 and d2) in a dose-dependent manner (Figure 2e1 and e2; IC_{50} of MFA on the NVDC at 0 mM glucose is 31 μM; $n=5$; at 2.8 mM glucose is 27 μM), respectively. In contrast, MFA had no effect on the voltage-dependent conductance that consistently appeared in the presence of high glucose (Figure 2d3 and e3). These results suggested that MFA depolarized INS-1cells by inhibiting the glucose-sensitive NVDC.

MFA blocks K_{ATP} through an extracellular mechanism

To further study this glucose-sensitive NVDC, we made perforated patch voltage-clamp recordings in INS-1 cells and analysed transmembrane conductances of the same cell in the presence of 145 mM of extracellular NaCl or KCl, respectively (both solutions were glucose-free). When the extracellular Na^+ was replaced with K^+, the reversal potential for the glucose-sensitive NVDC shifted from

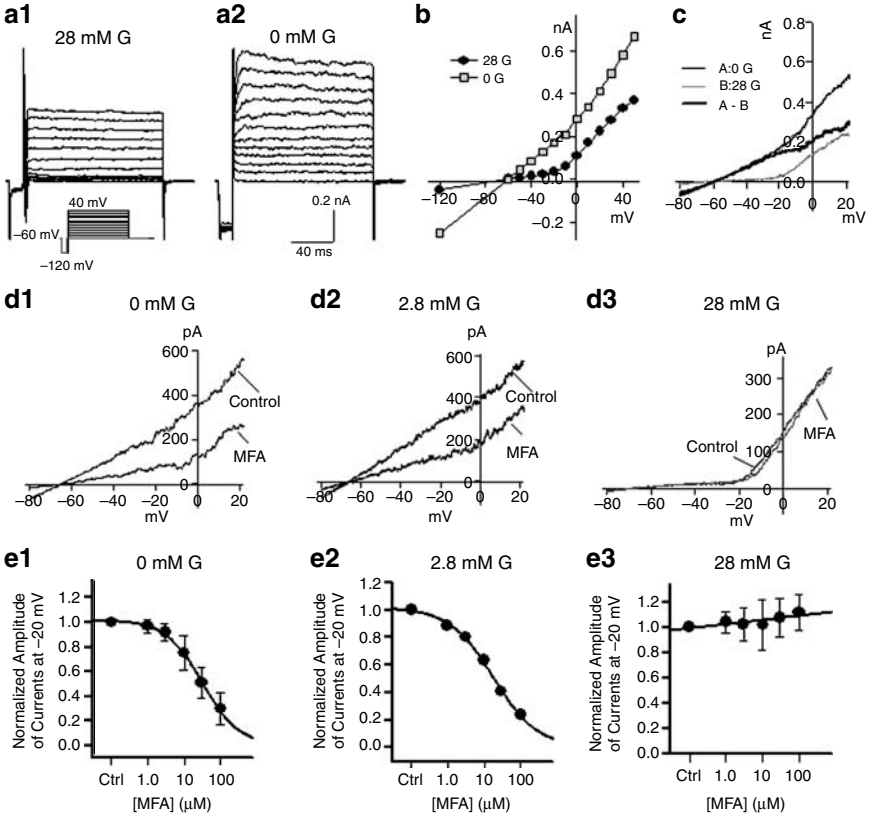

Figure 2 MFA inhibits an NVDC that appears at low concentrations of glucose. All results shown in the figure were obtained by perforated patch recordings. (**a**) Typical traces of transmembrane currents evoked by changing V_M with voltage-steps at 28 mM glucose (**a1**) and 0 mM glucose (**a2**), respectively, in the same cell. The inset in (**a1**) illustrates the V_M-changing protocol. (**b**) Current–voltage (*I–V*) curves obtained by plotting the current (measured at 10 ms of the hyperpolarizing step of the first voltage-change swipe, and at 80 ms of each depolarizing step) against the voltage, at 0 or 28 mM glucose. Note that currents increase independently of the V_M in the presence of 0 mM glucose, suggesting the development of an NVDC. (**c**) Shown are example *I–V* curves evoked by changing the V_M using a voltage-ramp protocol. The curves were obtained from tests in the same cells at 0 and 28 mM glucose, respectively. The component of whole cell current mediated by the NVDC (dark trace) is isolated by subtracting the *I–V* curve at 28 mM glucose from the *I–V* curve at 0 mM glucose. This NVDC displays a linear *I–V* relationship. (**d**) MFA (100 μM) inhibits the NVDC that appears in cells bathed in 0 mM glucose (**d1**) and 2.8 mM *G* (**d2**). MFA (100 μM) has no effect on transmembrane current when the cell is exposed to high (28 mM) glucose (**d3**). (**e**) Dose–response curves showing the effect of MFA (1–100 μM) on transmembrane currents evoked in cells incubated with solution with 0 (**e1**), 2.8 (**e2**) and 28 mM glucose (**e3**). The currents were measured at -20 mV, because at this V_M, the voltage-dependent current is small. The amplitudes of currents are normalized to the control (before addition of MFA).

approximately -63 to about 0 mV (Figure 3a), suggesting that this NVDC is mediated by a K^+ channel. Moreover, under the same recording conditions, this non-voltage-dependent K^+ conductance was suppressed by addition of MFA to the ECS (Figure 3b and c; in MFA: $27 \pm 1.2\%$ of the control, $n = 4$ cells; $P < 0.01$).

The results described above strongly suggested that MFA stimulated INS-1 cells by inhibiting the K_{ATP} channel. To confirm this, we made conventional whole cell voltage-clamp recordings using patch electrodes filled with 150 mM KCl together with or without ATP (4 mM), and measured the voltage-step-evoked currents 10 min after whole cell configuration. Analyses showed that in the presence of intracellular ATP, a voltage-dependent outward conductance was observed in tested INS-1 cells (Figure 3d and g, $n = 26$). In contrast, in the absence of intracellular ATP, a NVDC gradually developed in all tested cells, regardless of extracellular glucose concentrations (Figure 3e and g, $n = 38$). When intracellular K^+ was replaced with the organic cation *N*-methyl-D-glucamine (NMDG, without intracellular ATP), the NVDC vanished along with the voltage-dependent outward current (Figure 3f and g), indicating that NVDC is mediated by K_{ATP} channels.

Under the same whole cell recording conditions (ICS contained 145 mM KCl without ATP), we employed the V-ramp protocol to study the progressive changes in the *I–V* relationship of the cells in response to the dilution of endogenous intracellular ATP. Results showed that immediately after whole cell configuration (about 10 s after the membrane rupture), only the voltage-dependent outward conductance could be seen (Figure 3h). The NVDC gradually appeared and developed fully within 4–6 min after whole cell configuration. Addition of MFA (100 μM) to the ECS reduced the amplitude (at -20 mV) of ATP-sensitive NVDC (Figure 3h and k). Remarkably, this ATP-sensitive NVDC was completely eliminated by adding the K_{ATP} channel blocker glibenclamide (5 μM) to the bath solution (Figure 3i). Including 5 μM of glibenclamide in the ICS also prevented the development of the NVDC (not shown), confirming that this NVDC is mediated by K_{ATP} channels. In the presence of this high

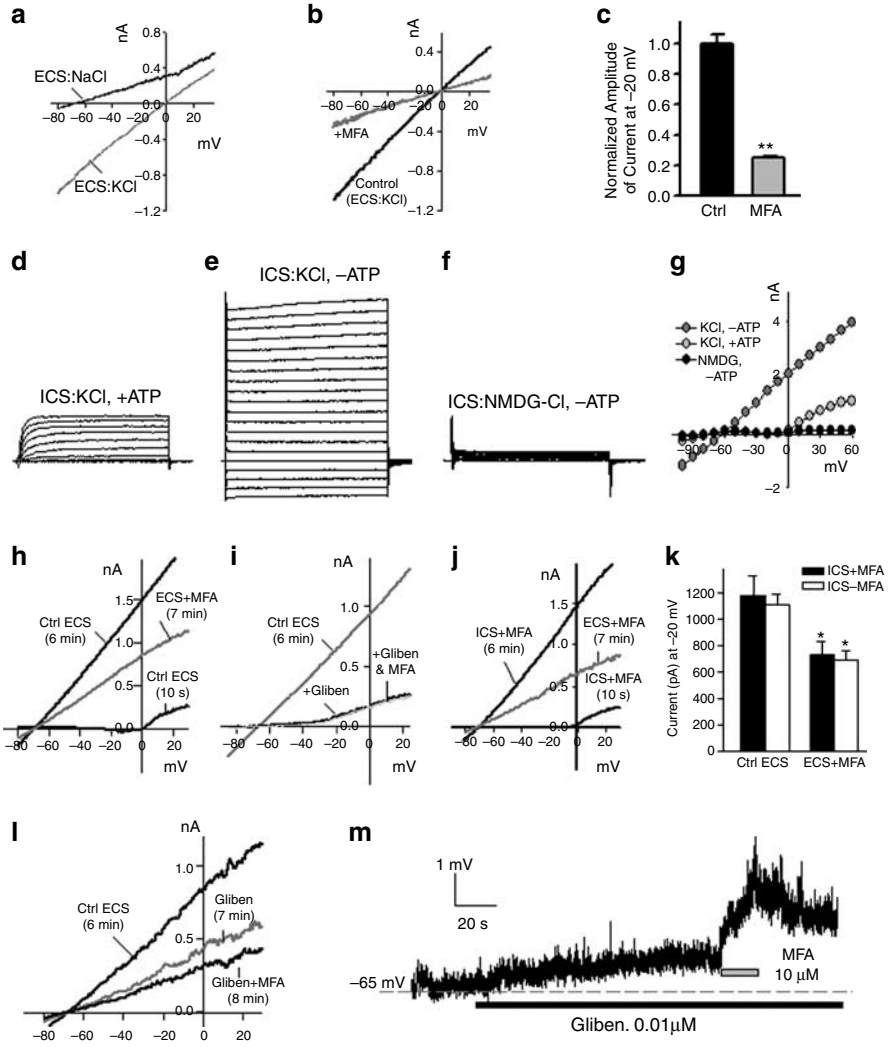

Figure 3 MFA inhibits K_{ATP}. Results shown in (**a** and **b**) of this figure were obtained by perforated patch recordings. (**a**) Plotted are the *I–V* curves showing the 'isolated' NVDC component by subtracting the whole cell transmembrane current at 28 mM glucose (*G*) from the current at 0 mM *G*. Currents were evoked in the same cell when it was bathed in glucose-free ECS that contain 145 mM NaCl or 145 mM KCl, respectively. Note that the reverse potential of the transmembrane current shifted from approximately −62 to about 0 mV when the extracellular Na^+ was replaced with K^+, indicating that the glucose-sensitive NVDC is mediated by a K^+ channel. (**b**) In the presence of 145 mM KCl (glucose-free), the non-voltage-dependent K^+ current was significantly inhibited by adding 100 μM of MFA to the bath. (**c**) Summary of the effects of MFA (100 μM) on the non-voltage-dependent K^+ current ($n=4$; $^{**}P<0.01$). (**d–f**) Conventional whole cell recordings were performed in INS-1cells that were bathed in solution containing 145 mM NaCl and 28 mM glucose, with patch-electrode filled with ICS containing 150 mM KCl and 4 mM ATP (**d**), or with 150 mM KCl but no ATP (**e**), or 150 mM NMDG-Cl but no ATP (**f**), respectively. (**g**) The voltage-step evoked currents shown in (**d–f**) were plotted against depolarizing voltages. (**h**) Plotted are the V-ramp evoked currents in the same cells under whole cell recording with control (Ctrl) ICS that contained 145 mM KCl without ATP. The currents shown in the graph were obtained at different time points after whole cell configuration. Note that the NVDC fully developed 6 min after whole cell configuration, and that 100 μM of MFA decreased the NVDC. (**i**) Application of 5 μM of glibenclamide eliminated the ATP-sensitive NVDC in INS-1 cell. In the presence of high glibenclamide, 100 μM of MFA failed to further affect the membrane conductance. (**j**) Without intracellular ATP, the NVDC readily developed in the presence of intracellular MFA (300 μM). Extracellular addition of MFA (100 μM) significantly decreased the NVDC. (**k**) Summary of the effects of MFA in ECSs and/or ICSs on NVDC. MFA (100 μM) in ECS reduced the NVDC ($n=11$–12; $^{*}P<0.001$ vs control ECS), regardless of the MFA content of ICS. However, MFA in ICS did not affect NVDC ($n=12$; $P>0.05$). (**l**) Low concentrations (0.01 μM) of glibenclamide decreased the ATP-sensitive NVDC. In this condition, addition of MFA (10 μM) to the bath further reduced the current. (**m**) Low concentrations (0.01 μM) of glibenclamide slightly depolarizes INS-cells. Under this condition, addition of MFA (10 μM) depolarized the cell further.

concentration of glibenclamide, MFA failed to further reduce the voltage-dependent conductance (Figure 3i). Together, these results firmly indicated that MFA excites INS-1 cells by inhibiting the K_{ATP} activity.

MFA inhibits intracellular COX. To examine whether MFA affect K_{ATP} function indirectly via an intracellular mechanism, we included 300 μM of MFA in ICS, and measured the amplitude of the V-ramp evoked currents 10 min after whole cell configuration. Notably, with 300 μM MFA in ICS, the K_{ATP}-mediated NVDC showed amplitudes comparable to the controls (Figure 3j and k). Under this condition, however, addition of 100 μM of MFA to the bath

solution could significantly reduce the K_{ATP}-mediated NVDC (Figure 3j and k). In addition, under whole cell current clamp recordings, including 300 μM MFA in the ATP-free ICS failed to induce membrane depolarization, whereas addition of 100 μM of MFA to the ECS caused a large depolarization (not shown). These results indicated that MFA blocks the K_{ATP} through an extracellular mechanism.

Sulphonylureas reduce K_{ATP} activity by binding to an intracellular domain of SURs of the channel. We examined whether sulphonylurea and MFA could additively inhibit K_{ATP} when the sulphonylurea was at subthreshold concentrations (at which the K_{ATP} was not completely inhibited). Application of 0.01 μM of glibenclamide to the bath reduced the amplitude of the K_{ATP}-mediated NVDC (Figure 3l) by $43 \pm 13\%$ of controls ($n = 4$). In the presence of this low concentration of glibenclamide, addition of 10 μM of MFA further decreased the K_{ATP} current (Figure 3l) by $31 \pm 8\%$ of the control ($n = 3$). In addition, when a mild depolarization was induced in INS-1 cells by this low concentration of glibenclamide, 10 μM of MFA could readily depolarize the cell further (Figure 3m), indicative of an additive effect.

MFA depolarizes primary beta cells isolated from mouse islets

We then examined the effect of MFA on the excitability of primary beta cells that were isolated from the MIP-GFP mouse. Specifically, perforated patch current-clamp recordings were performed in these GFP-expressing primary cells under fluorescent microscope. Application of MFA dose-dependently depolarized the primary beta cells bathed in 2.8 mM glucose (Figure 4a), but not in 16.8 mM glucose (Figure 4b). The EC_{50} for MFA to stimulate primary beta cells was 26 μM ($n = 5$) (Figure 4c), similar to that in INS-1 cells (see Figure 1g). Under whole cell voltage-clamp conditions, the primary beta cells generated a voltage-dependent conductance in the presence of intracellular ATP (Figure 4d1 and d3). A non-voltage-gated outward conductance that was reversed about -63 mV was consistently observed when ATP was omitted from ICS (Figure 4d2 and d3), suggestive of a K_{ATP} current. Focal application of MFA (30 μM) to the cells reduced the K_{ATP} current (Figure 4e and f). Also, MFA depolarized the primary beta cells under whole cell current-clamp recordings with ATP-free ICS (Figure 4g). These results demonstrated that MFA indeed stimulates primary beta cells by blocking K_{ATP} channels.

Stimulation of INS-1 cells by other NSAIDs

To examine whether other NSAIDs also block K_{ATP}, we also made perforated patch recordings in INS-1 cells, in the presence of low and high extracellular glucose, and tested the effects of FFA and ASA on the V_M and voltage-change-evoked currents. The data showed that under current-clamp recordings, both FFA (Figure 5a) and ASA (Figure 5c)

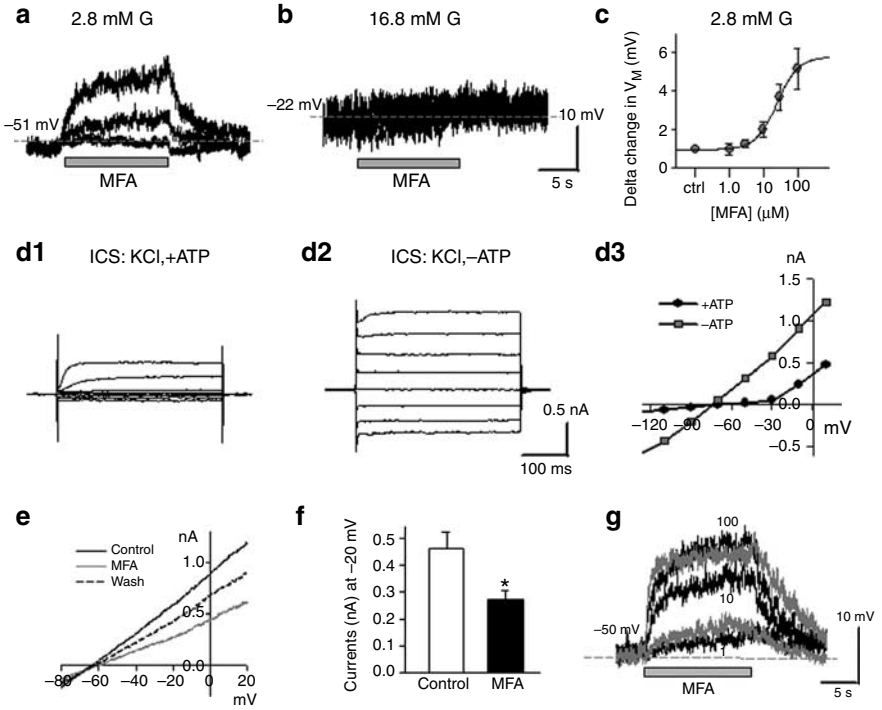

Figure 4 MFA depolarizes isolated pancreatic beta cells via inhibiting K_{ATP} channels. In perforated patch recordings, MFA dose-dependently depolarizes pancreatic beta cells in the presence of 2.8 mM glucose (**a** and **c**), but not at 16.8 mM glucose (**b**). (**d**) Currents evoked by depolarizing voltage steps (from -100 to 20 mV with 20 mV interval) in pancreatic beta cells under conventional whole cell recordings (ICS contains 145 mM KCl, without ATP) at the 10th second (**d1**) and the 3rd min (**d2**) after whole cell configuration. The currents illustrated in (**d1**) and (**d2**) are plotted against voltage steps (**d3**), demonstrating the development of K_{ATP} conductance in the cell. (**e**) In whole cell voltage-clamp recordings, V-ramp reveals the non-voltage-dependent K_{ATP} current, which is reversibly inhibited by MFA (100 μM). (**f**) Summary of the effects of MFA (100 μM) on the amplitude (at -20 mV) of K_{ATP} currents ($n = 5$; $P < 0.05$). (**g**) Typical traces show that under whole cell current clamp conditions, MFA (1–100 μM) dose-dependently induced depolarization in a pancreatic beta cell.

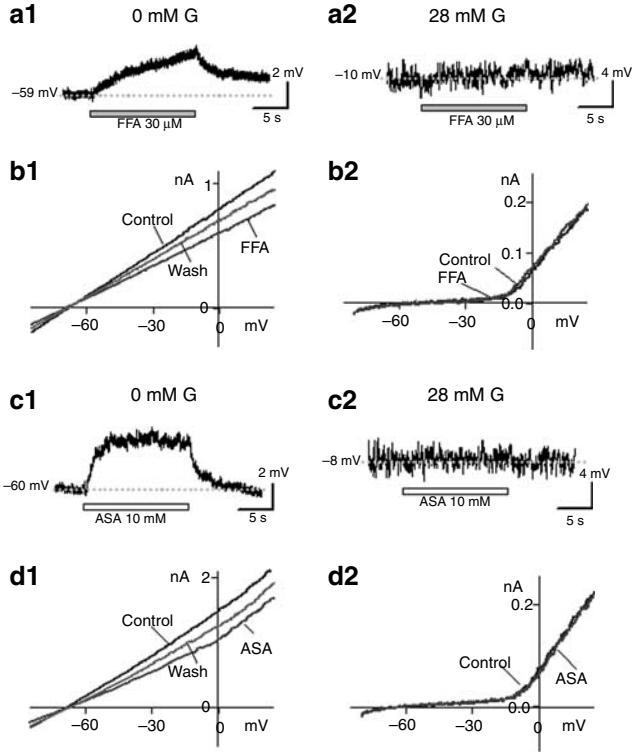

Figure 5 FFA and ASA also stimulate INS-1 cells by inhibiting K_{ATP}. Data in this figure are typical results obtained by perforated patch recordings in INS-1 cells. (**a**) FFA depolarizes INS-1 cell in the presence of low glucose (**a1**), but not at high glucose (**a2**). (**b**) FFA inhibits K_{ATP} in the presence of low glucose (**b1**), but not at high glucose (**b2**). (**c**) ASA depolarizes INS-1 cells in the presence of low glucose (**c1**), but not at high glucose (**c2**). (**d**) ASA inhibits K_{ATP} in the presence of low glucose (**d1**), but not at high glucose (**d2**).

depolarized the cell in the presence of low glucose but not high glucose. Under voltage-clamp recording mode, the amplitude (at −20 mV) of the NVDC was reduced by FFA (Figure 5b; to 73±3% of the control; $n=4$; $P<0.05$) and ASA (Figure 5d; to 79±3% of the control, $n=4$; $P<0.05$) in the presence of low glucose but not the voltage-dependent conductance at high glucose. These data suggested that, like MFA, some other NSAIDs also inhibit the K_{ATP} channel in beta cells.

MFA elevates intracellular [Ca^{2+}] of INS-1 cells and increases insulin secretion

Membrane depolarization of pancreatic beta cells causes Ca^{2+}-entry through voltage-gated Ca^{2+} channels, and consequently induces insulin secretion. We examined the effect of MFA on intracellular Ca^{2+} concentration ($[Ca^{2+}]_i$) of INS-1 cells in the presence of 2.8 and 28 mM of glucose, respectively. Live-cell imaging illustrated that in the presence of 2.8 mM glucose, $[Ca^{2+}]_i$ remained at relatively low levels. Application of MFA (30 μM) rapidly elevated $[Ca^{2+}]_i$ (Figure 6a, upper row). Adding the L-type Ca^{2+}-channel blocker nifedipine (10 μM) to the bath solution lowered $[Ca^{2+}]_i$. Notably, in the presence of nifedipine, MFA (30 μM) failed to increase $[Ca^{2+}]_i$ (Figure 6a, middle row), indicating that MFA induced Ca^{2+}-entry through the voltage-gated Ca^{2+}-channels. In contrast, the basal $[Ca^{2+}]_i$ of the cells at 28 mM of glucose was significantly higher than that at low glucose (Figure 6a, lower row). Application of MFA (30 μM) had no significant effect on $[Ca^{2+}]_i$ in the cells that were bathed in 28 mM glucose.

We then determined insulin secretion from INS-1 cells in the absence and presence of different concentrations (1.0–1000 μM) of MFA. Insulin release from the INS-1 cells was significantly stimulated by 28 mM of glucose (Figure 6b, right panel), compared to those from cells bathed in 0 mM (Figure 6b, left panel) or 2.8 mM (Figure 6b, middle panel) of glucose. Remarkably, MFA dose-dependently increased the insulin secretion of INS-1 cells at 0 and 2.8 mM glucose (Figure 6b, left and middle panels), but not at 28 mM glucose (Figure 6b, right panel). This result demonstrated that MFA increases insulin secretion in the presence of low glucose.

Discussion and conclusions

This study mainly examined the effects of the NSAID, MFA, on the excitability of cultured pancreatic beta cells and insulin secretion from INS-1 cells, as well as the underlying mechanism for the actions of this drug. We found that low dose (1.0 μM) MFA excites beta cells by inhibiting the K_{ATP} channel activity, thus increasing insulin secretion. In addition, our results suggested that MFA inhibits the K_{ATP} channel through an extracellular mechanism. These findings may explain, at least partially, the hypoglycaemic side effect of certain clinically used NSAIDs.

One of the principal findings was that MFA depolarized INS-1 cells only when the extracellular glucose was low. This suggests that MFA targets a molecule involving glucose metabolism. In this regard, a previous study had proposed that MFA inhibits the K_{ATP} channel because it blocked the *in vivo* cardioprotective effect of cromakalim, a K_{ATP} channel opener (Grover *et al*., 1994). Since the subunit composition of K_{ATP} channels in beta cells differs from channels expressed in cardiomyocytes, it was necessary to determine whether MFA also modified the function of K_{ATP} channels in beta cells. In particular, MFA and other fenamates exhibit complex actions on diverse molecules. For example, fenamates exert anti-inflammatory effects via inhibition of COX, an enzyme that catalyses the biosynthesis of prostaglandins (PGs) from arachidonic acid (AA). In relation to this theme, AA activates large-conductance Ca^{2+}-activated K^+ channels (BK_{Ca}) (Lu *et al*., 2005), and PGs activate K_{ATP} channels by activating protein kinase C (Hide *et al*., 1995). Therefore, MFA could indirectly affect these ion channels through regulating COX activity. In addition, fenamates directly modulate BK_{Ca} channels (Ottolia and Toro, 1994), $GABA_A$ receptor-gated Cl^- channels (Woodward *et al*., 1994), KCNQ2/Q3 K^+ channels (Peretz *et al*., 2005) and voltage-gated Kv2.1 channels (Lee and Wang, 1999). Given that pancreatic beta cells express some of these channels, known as targets for the fenamates, including K_{ATP} (Nichols, 2006), $GABA_A$ receptor (Dong *et al*., 2006) and Kv2.1 (MacDonald *et al*., 2002), the present study carried out serial experiments

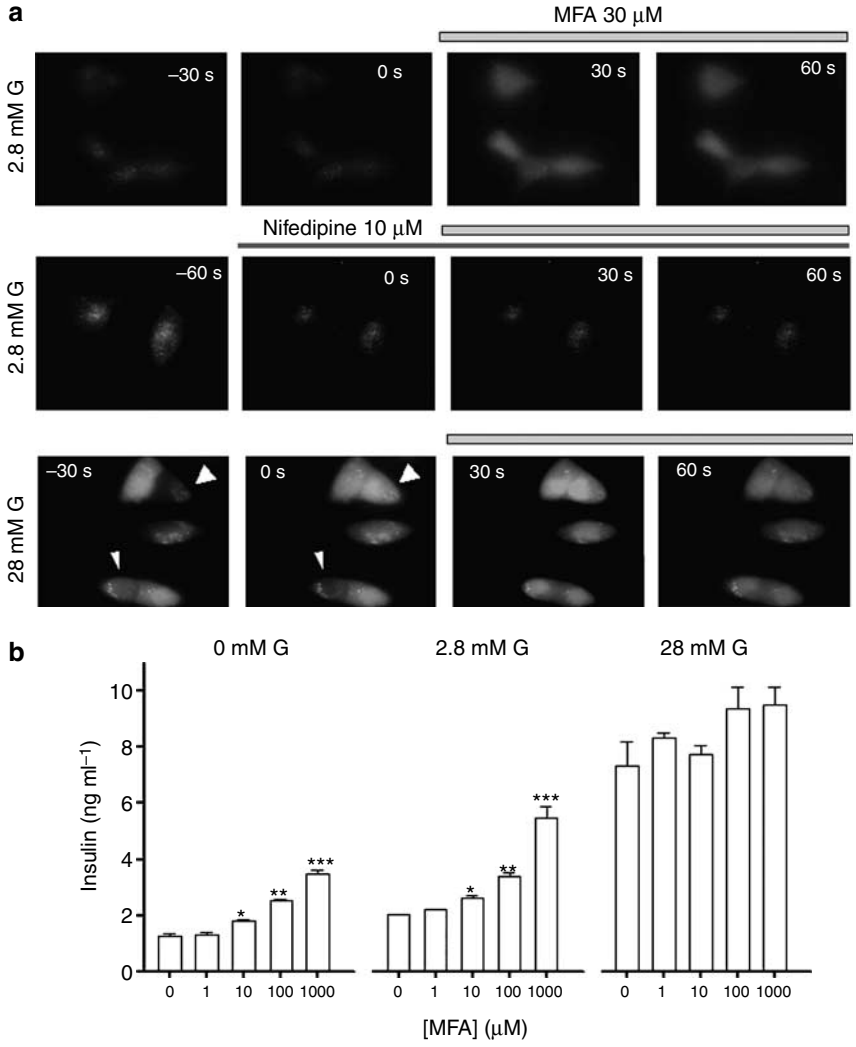

Figure 6 MFA elevates $[Ca^{2+}]_i$ in INS-1 cells and increases insulin release from the cells. (**a**) Typical Ca^{2+} fluorescence images obtained from the INS-cells. The basal level of $[Ca^{2+}]_i$ is significantly lower in cells bathed in ECS containing 2.8 mM glucose (the upper row, left two images) than that in cells at 28 mM glucose (the lower row, left two images). Note: under control conditions, $[Ca^{2+}]_i$ in certain cells fluctuates in the presence of high glucose (indicated by arrow heads). Application of MFA (30 μM, open bar) greatly increases $[Ca^{2+}]_i$ in cells bathed in low glucose (upper row) (normalized intensity of $[Ca^{2+}]_i$ at 2.8 mM glucose, control: 1.00 ± 0.25; +MFA: 6.44 ± 0.83; $n=4$; $P<0.01$), but not in cells at high glucose (lower row) (normalized intensity of $[Ca^{2+}]_i$ at 28 mM glucose, control: 8.26 ± 0.65; +MFA: 8.99 ± 0.82; $n=4$; $P>0.05$). Including the L-type Ca^{2+}-channel blocker nifedipine in the bath (solid black bar) for 2 min decreases $[Ca^{2+}]_i$ (see middle row, left two images). In the presence of nifedipine, MFA (30 μM) failed to increase $[Ca^{2+}]_i$. (**b**) MFA dose-dependently increases insulin release from INS-1 cells in the presence of low (0 and 2.8 mM) but not in high glucose (28 mM). *$P<0.05$; **$P<0.01$; ***$P<0.005$ in comparison to the control.

to identify the molecular target, through which MFA affects the function of beta cells.

Our electrophysiological results indicated that MFA excites the beta cells, including primary beta cells from mouse islets, primarily by inhibiting the K_{ATP} channel. Our results confirm the previous assumption that MFA is an inhibitor of the K_{ATP} channel (Grover *et al.*, 1994). It is worth emphasizing that high concentrations of MFA in the patch-electrode solution failed to inhibit K_{ATP} channel activity. This result demonstrates that MFA inhibits the K_{ATP} channels independently of COX activity and via an extracellular mechanism. Recent studies show that sulphonylurea-sensitive K_{ATP} channels are also located in various intracellular sites including secretory granules, mitochondria, endoplasmic reticulum and nucleus (Quesada and Soria, 2004). Regardless of the roles of these K_{ATP} channels in intracellular organelles in cell biology, our result implies that the MFA-induced rapid excitation in beta cells may not involve these intracellular K_{ATP} channels.

The voltage-gated Kv2.1 channels are expressed in pancreatic beta cells and blocking these channels enhances insulin secretion (MacDonald *et al.*, 2002). It is reported that MFA blocks Kv2.1 channels in neuronal cells with an estimated IC_{50} of 56 μM (Lee and Wang, 1999). We found that MFA did not induce depolarization in INS-1 cells in high glucose conditions, under which the voltage-dependent K^+-conductance was active (see Figure 2a1 and b). In addition, when the K_{ATP} conductance was eliminated by saturating concentrations of glibenclamide, high concentrations of MFA failed to further reduce the voltage-dependent

component. These data suggest that it is unlikely that MFA substantially stimulated the beta cells through blocking Kv2.1 channels.

Inhibition of K_{ATP} channels results in depolarization of pancreatic beta cells, and consequently leading to Ca^{2+}-entry through voltage-gated Ca^{2+} channels and insulin release. Indeed, MFA elevated the $[Ca^{2+}]_i$ and increased insulin secretion in the presence of low, but not high glucose. In addition, we found that in the presence of 0.1% of albumin, low concentrations (10 μM) of MFA significantly increased insulin secretion from INS-1 cells *in vitro*. It is apparent that further studies are necessary to clarify at what clinical doses fenamates affect insulin secretion from pancreatic beta cells *in vivo*. With respect to *in vivo* insulin secretion, effects of acute administration of salicylate compounds have been controversial in different studies (Garcia *et al*., 1984; van Haeften *et al*., 1991). It is possible that the prestimulus glucose levels may regulate subsequent insulin release (Giugliano *et al*., 1985). Recent studies indicate that insulin resistance in diabetics results from hepatic activation of inhibitory kappa B kinase (IKK-β) and nuclear factor-kappa B (Yuan *et al*., 2001) and high doses of salicylates inhibit IKK-β activity and might therefore ameliorate insulin resistance and improve glucose tolerance in type II diabetic patients (Yuan *et al*., 2001; Hundal *et al*., 2002). This study reveals that application of ASA also induced rapid membrane depolarization by blocking K_{ATP} channels in a glucose concentration-dependent manner. Whether this acute action of ASA contributed to its glucose-lowering effect remains to be established.

The glucose concentration-dependent effect of MFA on insulin release may explain the phenomenon that certain NSAIDs have side effects of inducing hypoglycemia (Sone *et al*., 2001) in diabetic patients who receive sulphonylurea therapy, but do not influence the glucose-induced hyperinsulinaemia or the glucose disappearance rate (Byford and Furman, 1985). Our data show that fenamates reduce the K_{ATP} channel thorough an extracellular mechanism, whereas sulphonylureas inhibit K_{ATP} channels by binding to intracellular domain of SURs. We reason that NSAIDs and sulphonylureas may restrain the channel activity in a synergistic manner. The risk of NSAID-induced hypoglycemia should be considered when glucose-lowering compounds are administered.

Acknowledgements

We thank Dr Manami Hara for providing the MIP-GFP transgenic mice and thank Dr Yi Zhang for the help in isolation of pancreatic beta cells. We also thank Dr Michael Jackson for the comments on the manuscript. This work is supported by the operating grant from Canadian Institutes of Health Research (MOP-74653) to WYL (MOP-79534) to QW, and MOP-49521 to MBW.

Conflict of interest

The authors state no conflict of interest.

References

Baron SH (1982). Salicylates as hypoglycemic agents. *Diabetes Care* **5**: 64–71.

Best L (2002). Study of a glucose-activated anion-selective channel in rat pancreatic beta cells. *Pflugers Arch* **445**: 97–104.

Best L (2005). Glucose-induced electrical activity in rat pancreatic beta cells: dependence on intracellular chloride concentration. *J Physiol* **568**: 137–144.

Byford AJ, Furman BL (1985). Lack of effect of BW755c on glucose-induced insulin secretion in the rat *in-vivo*. *J Pharm Pharmacol* **37**: 839–840.

Dai FF, Zhang Y, Kang Y, Wang Q, Gaisano HY, Braunewell KH *et al.* (2006). The neuronal Ca^{2+} sensor protein visinin-like protein-1 is expressed in pancreatic islets and regulates insulin secretion. *J Biol Chem* **281**: 21942–21953.

Dong H, Kumar M, Zhang Y, Gyulkhandanyan A, Xiang YY, Ye B *et al.* (2006). Gamma-aminobutyric acid up- and downregulates insulin secretion from beta cells in concert with changes in glucose concentration. *Diabetologia* **49**: 697–705.

Garcia C, Roncero I, Tamarit-rodriguez J, Tamarit J (1984). Effects of salicylate on insulin and glucagon secretion by the isolated and perfused rat pancreas. *Rev Esp Fisiol* **40**: 477–481.

Gilgore SG, Rupp JJ (1961). Response of blood glucose to intravenous salicylate. *Metabolism* **10**: 419–421.

Giugliano D, Ceriello A, Saccomanno F, Quatraro A, Paolisso G, D'onofrio F (1985). Effects of salicylate, tolbutamide, and prostaglandin E2 on insulin responses to glucose in noninsulin-dependent diabetes mellitus. *J Clin Endocrinol Metab* **61**: 160–166.

Gloyn AL, Siddiqui J, Ellard S (2006). Mutations in the genes encoding the pancreatic beta-cell KATP channel subunits Kir6.2 (KCNJ11) and SUR1 (ABCC8) in diabetes mellitus and hyperinsulinism. *Hum Mutat* **27**: 220–231.

Grover GJ, D'alonzo AJ, Sleph PG, Dzwonczyk S, Hess TA, Darbenzio RB (1994). The cardioprotective and electrophysiological effects of cromakalim are attenuated by meclofenamate through a cyclooxygenase-independent mechanism. *J Pharmacol Exp Ther* **269**: 536–540.

Hara M, Wang X, Kawamura T, Bindokas VP, Dizon RF, Alcoser SY *et al.* (2003). Transgenic mice with green fluorescent protein-labeled pancreatic beta-cells. *Am J Physiol Endocrinol Metab* **284**: E177–E183.

Harks EG, Deroos AD, Peters PH, Dehaan LH, Brouwer A, Yper DL *et al.* (2001). Fenamates: a novel class of reversible gap junction blockers. *J Pharmacol Exp Ther* **298**: 1033–1041.

Hide EJ, Ney P, Piper J, Thiemermann C, Vane JR (1995). Reduction by prostaglandin E1 or prostaglandin E0 of myocardial infarct size in the rabbit by activation of ATP-sensitive potassium channels. *Br J Pharmacol* **116**: 2435–2440.

Hundal RS, Petersen KF, Mayerson AB, Randhawa PS, Inzucchi S, Shoelson SE *et al.* (2002). Mechanism by which high-dose aspirin improves glucose metabolism in type 2 diabetes. *J Clin Invest* **109**: 1321–1326.

Kawajiri M, Okano Y, Kuno M, Tokukara D, Hase Y, Inada H *et al.* (2006). Unregulated insulin secretion by pancreatic beta cells in hyperinsulinism/hyperammonemia syndrome: role of glutamate dehydrogenase, ATP-sensitive potassium channel, and nonselective cation channel. *Pediatr Res* **59**: 359–364.

Kinard TA, Satin LS (1995). An ATP-sensitive Cl^- channel current that is activated by cell swelling, cAMP, and glyburide in insulin-secreting cells. *Diabetes* **44**: 1461–1466.

Kubacka RT, Antal EJ, Juhl RP, Welshman IR (1996). Effects of aspirin and ibuprofen on the pharmacokinetics and pharmacodynamics of glyburide in healthy subjects. *Ann Pharmacother* **30**: 20–26.

Lee YT, Wang Q (1999). Inhibition of hKv2.1, a major human neuronal voltage-gated K^+ channel, by meclofenamic acid. *Eur J Pharmacol* **378**: 349–356.

Lu T, Wang XL, He T, Zhou W, Kaduce TL, Katusic ZS *et al.* (2005). Impaired arachidonic acid-mediated activation of large-conductance Ca^{2+}-activated K^+ channels in coronary arterial smooth muscle cells in Zucker Diabetic Fatty rats. *Diabetes* **54**: 2155–2163.

Macdonald PE, Sewing S, Wang J, Joseph JW, Smukler SR, Sakellaropoulos G *et al.* (2002). Inhibition of Kv2.1 voltage-dependent K^+

channels in pancreatic beta cells enhances glucose-dependent insulin secretion. *J Biol Chem* **277**: 44938–44945.
Nichols CG (2006). KATP channels as molecular sensors of cellular metabolism. *Nature* **440**: 470–476.
Ottolia M, Toro L (1994). Potentiation of large conductance KCa channels by niflumic, flufenamic, and mefenamic acids. *Biophys J* **67**: 2272–2279.
Peretz A, Degani N, Nachman R, Uziyel Y, Gibor G, Shabat D *et al*. (2005). Meclofenamic acid and diclofenac, novel templates of KCNQ2/Q3 potassium channel openers, depress cortical neuron activity and exhibit anticonvulsant properties. *Mol Pharmacol* **67**: 1053–1066.
Qian F, Huang P, Ma L, Kuznetsov A, Tamarina N, Philipson LH (2002). TRP genes: candidates for nonselective cation channels and store-operated channels in insulin-secreting cells. *Diabetes* **51** (Suppl 1): S183–S189.
Quesada I, Soria B (2004). Intracellular location of KATP channels and sulphonylurea receptors in the pancreatic beta-cell: new targets for oral antidiabetic agents. *Curr Med Chem* **11**: 2707–2716.
Reid J, Macdougall AI, Andrews MM (1957). Aspirin and diabetes mellitus. *Br Med J* **33**: 1071–1074.
Solimena M (1998). Vesicular autoantigens of type 1 diabetes. *Diabetes Metab Rev* **14**: 227–240.
Sone H, Takahash A, Yamada N (2001). Ibuprofen-related hypoglycemia in a patient receiving sulfonylurea. *Ann Intern Med* **134**: 344.
Sugita M, Hirono C, Shiba Y (2004). Gramicidin-perforated patch recording revealed the oscillatory nature of secretory Cl^- movements in salivary acinar cells. *J Gen Physiol* **124**: 59–69.
Van haeften TW, Veneman TF, van der Veen EA (1991). Influence of lysine acetyl-salicylate on glucose and arginine stimulated insulin release in man. *Horm Metab Res* **23**: 168–170.
Wang Q, Li L, Xu E, Wong V, Rhodes C, Brubaker PL (2004). Glucagon-like peptide-1 regulates proliferation and apoptosis via activation of protein kinase B in pancreatic INS-1 beta cells. *Diabetologia* **47**: 478–487.
Woodward RM, Polenzani L, Miledi R (1994). Effects of fenamates and other nonsteroidal anti-inflammatory drugs on rat brain GABAA receptors expressed in *Xenopus* oocytes. *J Pharmacol Exp Ther* **268**: 806–817.
Yuan M, Konstantopoulos N, Lee J, Hansen L, Li ZW, Karin M *et al*. (2001). Reversal of obesity- and diet-induced insulin resistance with salicylates or targeted disruption of Ikkbeta. *Science* **293**: 1673–1677.